Published in final edited form as:
Acta Biomater. 2012 October ; 8(10): 3754–3764. doi:10.1016/j.actbio.2012.06.028.

Variations in chondrogenesis of human bone marrow-derived mesenchymal stem cells in fibrin/alginate blended hydrogels

Kun Ma[a,*], **Ashley L. Titan**[a], **Melissa Stafford**[a], **Chun hua Zheng**[a], and **Marc E. Levenston**[a,*]
[a]Department of Mechanical Engineering, Stanford University, Stanford, CA 94305, USA

Abstract

Fibrin and alginate hydrogels have been widely used to support chondrogenesis of bone marrow-derived mesenchymal stem cells (BM-MSCs) for articular cartilage and fibrocartilage tissue engineering, with distinct advantages and disadvantages to each material. Attempting to produce a gel scaffold exhibiting beneficial characteristics of both materials, we fabricated fibrin/alginate blended hydrogels at various blend ratios and evaluated the gel morphology, mechanical properties and their support for BM-MSC chondrogenesis. Results show that when the fibrin/alginate ratio decreased, the fibrin architecture transitioned from uniform to interconnected fibrous and finally to disconnected islands against an alginate background, with opposing trends in the alginate architecture. Fibrin maintained gel extensibility and promoted cell proliferation, while alginate improved the gel biostability and better supported glycosaminoglycan and collagen II production and chondrogenic gene expression. Blended gels had physical and biological characteristics intermediate between fibrin and alginate. Of the blends examined, FA 40:8 (40 mg/mL fibrinogen blended with 8 mg/mL alginate) was found to be the most appropriate group for future studies on tension-driven BM-MSC fibrochondrogenesis. As BM-MSC differentiation appeared to vary between fibrin and alginate regions of blended scaffolds, this study also highlighted the potential to develop spatially heterogeneous tissues through manipulating the heterogeneity of scaffold composition.

Keywords

Chondrogenesis; mesenchymal stem cells; fibrin; alginate; hydrogel

1. Introduction

Tissue engineering offers the potential to treat damaged or diseased tissues with functional replacements composed of biocompatible scaffolds seeded with appropriate cells [1]. However, there are significant challenges for developing fibrocartilaginous tissues with appropriate compositions and structures. Fibrocartilaginous organs such as the knee menisci are highly organized, heterogeneous tissues with macroscopic and microscopic heterogeneities in extracellular matrix (ECM) composition and cell phenotype. The radially

*Corresponding authors. 233 Durand Building, 496 Lomita Mall, Stanford, CA 94305-4038, USA. Tel.: +1 650 723 9464; fax: +1 650 725 1587, makun041210@gmail.com (K. Ma), levenston@stanford.edu (M.E. Levenston).

Disclosures
The authors have no conflicts of interest to disclose.

inner region of the meniscus has an ECM most similar to articular cartilage, with relatively high levels of collagen II and the large proteoglycan aggrecan, while its surface and outer regions have more fibrous ECM with lower levels of these components [2–5]. In the radially middle and outer regions, collagen II, aggrecan and other quantitatively minor ECM components are concentrated in the tie sheaths and the matrix compartment surrounding the primary circumferential collagen bundles [3, 6], producing a highly heterogeneous matrix architecture at the mesoscale. The cells are also spatially heterogeneous, with gradual radial variations in cell morphology [7] and gene expression profiles [8] from rounded, chondrocyte-like cells in the inner region to spread, fibroblast-like cells in the outer region. Disruption of this structure due to traumatic injury or age-related degradation may lead to altered joint biomechanics and the onset of osteoarthritis [9] but, like articular cartilage, meniscal fibrocartilage has a poor intrinsic repair capacity due to its limited vascularity [10].

Human bone marrow-derived mesenchymal stem cells (BM-MSCs) have been widely used for tissue repair or regeneration purpose due to their multi-lineage differentiation and self-renewal potentials [11, 12]. However, appropriate types or combinations of signals will be required to produce fibrochondrogenic differentiation with desired cell phenotype and ECM structures [13]. Preliminary studies indicate that combinations of fibrogenic and chondrogenic soluble factors may encourage development of a fibrochondrocytic phenotype by BM-MSCs *in vitro* [14]. Physical cues may also interact with soluble factors to influence MSC differentiation. The use of chondrogenic media in conjunction with natural cell-adhesive scaffolds (e.g., fibrin or gelatin) may induce fibrocartilaginous tissue formation [15]. Aligned nanofibrous topography induced fibrogenic differentiation of BM-MSCs that were cultured in chondrogenic medium [16], producing higher collagen I expression and lower aggrecan expression than developed in cell pellets on day 7. However, BM-MSCs cultured on aligned nanofibrous topography showed no proliferation and limited matrix production.

A variety of hydrogel scaffolds based on synthetic and natural polymers have been used for cartilage tissue engineering. The most commonly used class of synthetic hydrogels is based on poly(ethylene glycol) (PEG) or PEG-derivatives. Even when modified with bioactive additives, however, PEG-based hydrogels do not support chondrogenesis and cartilage-specific ECM production as well as some natural materials such as alginate and hyaluronic acid [17]. Commonly used natural hydrogels include fibrin, collagen, gelatin, alginate, agarose, hyaluronic acid and chitosan [15, 18]. Fibrin has been widely used in cartilage tissue engineering [19–21] as it can gel *in situ* to fill irregular defects and resemble the native healing clot formation. However, like collagen and gelatin gels, fibrin gels can shrink substantially during cell culture [15]. Alginate [22, 23] and agarose [24, 25], both derived from marine algae, have also been used in engineering cartilage tissue as they maintain the rounded chondrocyte morphology and a chondrocytic phenotype. The drawbacks of using these non-tissue derived polysaccharides include poor biodegradability [26]. However, compared to other gel materials, alginate offers the benefit of dissolving into monomer subunits using chelating agents, such as citrate [15], which facilitates the subsequent removal of the alginate component to circumvent the lack of resorbability [26].

Previous studies from our laboratory have shown the potential of inducing BM-MSCs into a fibrochondrogenic lineage in three-dimensional (3D) hydrogel system by applying cyclic tensile loading as a fibrogenic stimulus on bovine BM-MSCs cultured in chondrogenic medium [13]. One week of intermittent cyclic tension significantly stimulated collagen I mRNA expression in the constructs, and increased the total sulfated glycosaminoglycan (sGAG) and collagen contents as well as collagen alignment. In that study, fibrin hydrogel was used as a scaffold to support tensile loading of the developing construct due to its high extensibility and biocompatibility. However, unconstrained fibrin gels were found to shrink

substantially during culture, while constraining the gels increased the sGAG release to the media [13]. In contrast, alginate hydrogel is more dimensionally stable, but it is more brittle and easy to tear [17], making the tensile loading studies difficult. Alginate is expected to be more supportive of chondrogenic differentiation than fibrin due to the absence of adhesive domains that may inhibit chondrogenesis [27]. Therefore, in an attempt to balance the characteristics of the two materials, we explored the feasibility of blending fibrin and alginate at different ratios and evaluated their mechanical properties and support for BM-MSC chondrogenesis. This study aimed both to improve the gel properties for supporting future studies on BM-MSC fibrochondrogenesis involving tensile loading and to explore the use of blended hydrogels for the development of heterogeneous engineered tissues through manipulation of the scaffold composition.

2. Materials and Methods

2.1. Reagents

Unless otherwise stated, all reagents used in this study were purchased from Invitrogen (Carlsbad, CA). Human BM-MSCs that were harvested from healthy volunteer donors, expanded through one monolayer passage and characterized for cell surface markers, colony forming units and trilineage differentiation potential were provided by the Texas A&M Health Science Center, College of Medicine Institute for Regenerative Medicine at Scott & White through a grant from NCRR of the NIH, Grant # P40RR017447. Bovine fibrinogen, thrombin, aprotinin, Fast Green, bovine serum albumin (BSA), and Safranin-O were from Sigma-Aldrich (St. Louis, MO). Sodium alginate was from NovaMatrix FMC BioPolymer (Philadelphia, PA). Rabbit anti-human aggrecan G3 antibody and collagen II antibody were from Fisher Scientific (Rockford, IL) and Abcam (Cambridge, MA), respectively. Recombinant human transforming growth factor-β3 (TGF-β3) was from R&D Systems (Minneapolis, MN). ITS+ premix solution was from BD Biosciences (San Jose, CA). The RiboPure kit (Ambion®), the high capacity RNA-to-CDNA kit and fast SYBR® Green master mix were from Applied Biosystems (Foster City, CA).

2.2 Fabrication of fibrin/alginate blended hydrogels

Fibrinogen and alginate were dissolved in high glucose Dulbecco's modified Eagle's medium (DMEM) separately and mixed well to produce a range of final concentrations (Table 1). For convenience, the different blend groups are denoted by the ratio of fibrin to alginate in mg/mL (e.g., FA X:Y gels had final concentrations of X mg/mL fibrin and Y mg/mL alginate). Rectangular molds were used to cast acellular gels with dimensions of 4 mm thickness, 10 mm width, and 18 mm length for tensile tests. Cylindrical molds were used to cast gels 4 mm in diameter and 3 mm in height for all other studies. For fibrin-incorporating groups, thrombin was first added to the mold, followed by the addition of the fibrinogen/alginate solution. The fibrin was allowed to polymerize in a humidified incubator at 37 C for 50 min. The gels were then covered with sterile nylon filter paper, which was held in place with sterilized stainless steel clips, and immersed in 100 mM $CaCl_2$ for 50 min at room temperature to allow alginate cross-linking. In preliminary studies, we observed no effect of the alginate polymerization protocol on gel architecture, cell viability or sGAG accumulation for BM-MSCs in fibrin constructs, and similarly observed no effect of the fibrin polymerization protocol on gel architecture, cell viability or sGAG accumulation for BM-MSCs in alginate constructs. To facilitate comparison with other studies using fibrin or alginate alone, pure alginate gels were cross-linked without fibrin polymerization steps and pure fibrin gels were polymerized without alginate polymerization steps. For culture experiments, human BM-MSCs were monolayer-expanded through 5 passages using a low seeding density expansion protocol [28] and thoroughly mixed with the fibrinogen/alginate solutions to reach a final concentration of 20×10^6 cells/mL, followed immediately by gel

polymerization. Although we expect that the thorough mixing resulted in uniform cell distribution between components of the blended hydrogels and no obvious disparities in cellularity were obvious in freshly seeded constructs, we did not directly examine the uniformity of cell entrapment between the two components.

2.3. Distribution of fibrin and alginate in different gel groups

Acellular gels were fixed, dehydrated, embedded in paraffin and sectioned at 8μm with a rotating microtome (Microm HM355S). Sections were deparaffinized, hydrated, stained with 0.001% Fast Green solution for 5 min, rinsed quickly with 1% acetic acid solution for no more than 10–15 sec, and stained in 0.1% Safranin-O solution for 5 min. Sections were dehydrated, mounted, dried and viewed under an inverted microscope (Zeiss Invertoskop).

2.4. Tensile testing

Tensile tests for acellular gel specimens (4 mm thickness, 10 mm width) were performed with a microtester (model 5848, Instron, Norwood, MA) equipped with a 100 N load cell. The specimens were attached to custom grips with cyanoacrylate giving a final gauge length of 8 mm. The region between the grips (gauge region) was stretched to a final length of 20 mm at a stroke rate of 1.88 mm/min, recording load and extension data. The average engineering stress was calculated as the force divided by the original cross-sectional area, and the average engineering strain was calculated as the change in length divided by the gauge length. The ultimate tensile stress was determined as the greatest engineering stress achieved, and the critical strain was defined as the strain corresponding to the ultimate stress. The tensile modulus was determined via least squares regression as the slope of the linear region of the engineering stress-engineering strain curve from 45% to 75% of the ultimate tensile stress (R^2 0.99).

2.5. Gel culture

After gel polymerization, samples were washed in phosphate buffered saline (PBS) and cultured for 24 h in MSC growth medium consisting of αMEM plus 16.5% FBS and 2 mM L-glutamine for cell recovery [23]. Samples were then cultured for 28 days in chondrogenic medium consisting of high glucose DMEM supplemented with 10 ng/mL TGF-β3, 100 nM dexamethasone, 1% ITS+ Premix, 0.1 mM nonessential amino acids, 1% antibiotic/antimycotic, 50 μg/mL L-ascorbic acid-2-phosphate and 0.1 TIU/mL aprotinin, with medium changed and collected every other day. The use of a fibrinolytic inhibitor is generally necessary to stabilize fibrin scaffolds and prevent cell-mediated scaffold degradation in vitro [13, 29–31], and aprotinin has been found to minimally affect MSC behavior in fibrin constructs [31]. Additional acellular gels were maintained under comparable conditions.

2.6. Gel diameter measurement and biochemical assays

On days 0, 14 and 28, both cellular and acellular gels were collected for diameter measurement and biochemical assays. The gels were photographed against a metric ruler using a consistent camera setup and the gel diameter was measured five times per sample at different orientations with image analysis software (ImageJ, NIH, Bethesda, MD) and averaged for each sample. Each gel was weighed, lyophilized, reweighed, and digested with 0.5 mL 1mg/mL Proteinase K (supplemented with 100 mM EDTA in 100 mM ammonium acetate for alginate-incorporated gels) at 60°C overnight. The DNA contents were measured using the Hoechst dye assay [32] with calf thymus DNA standards. The sGAG contents of constructs and media samples were measured with the 1,9 dimethyl methylene blue (DMMB) assay (pH=1.5, absorbance at 595 nm) [33] with chondroitin sulfate standards after subtraction of the average background reading from the corresponding acelluar gel

groups. The cumulative sGAG released was determined on a sample-by-sample basis by summing the sGAG contents of collected media samples for that construct, and the total sGAG produced was determined by summing construct sGAG content and cumulative sGAG release.

2.7. Immunofluorescence imaging

Day 28 gel constructs were fixed with 10% neutral buffered formalin over night, rinsed with PBS, dehydrated and embedded in paraffin. Samples were subsequently sectioned at 8 μm onto glass slides, deparaffinized and rehydrated in water. Antigen retrieval was performed by incubating the samples in 0.1% trypsin (w/w) in PBS for 15 min at 37 °C for detecting collagen II or in 0.1 U/mL chondroitinase ABC for 1 hour at 37 °C for detecting aggrecan. Samples were then washed with PBS, blocked with 2% BSA and incubated with 10 μg/mL rabbit anti-human aggrecan G3 and 10 μg/mL collagen II antibodies overnight at 4°C, followed by washing and incubation with 10 μg/mL Alexa Fluor® 488 goat anti-rabbit secondary antibody for 1 hour at room temperature. To visualize the actin cytoskeleton, samples were incubated in 0.1% Triton-X for 10 min at room temperature, rinsed, blocked with 1% BSA, and then incubated in rhodamine-phalloidin solution for 20 min at room temperature. DNA was labeled with 4′,6-diamidino-2-phenylindole, dihydrochloride (DAPI). Negative controls without primary antibodies were stained in parallel. Slides were imaged using an Axiovert 200M fluorescence microscope (Carl Zeiss Light Microscopy, Germany).

2.8. Gene expression analysis

RNA was isolated from gel constructs using the Tri-spin method [34]. Briefly, RNA was extracted from the gels using the Trizol reagent and chloroform and precipitated with 100% ethanol. The RNA was further purified using the RiboPure kit according to the manufacturer's protocol. Total RNA was reverse transcribed to cDNA using the high capacity RNA-to-CDNA kit. Gene expression was measured by real-time RT-PCR using the fast SYBR® Green master mix and custom primers (Table 2). Genes examined included collagen IIa, aggrecan and the transcription factor Sox9, common chondrogenic markers, collagen X, a hypertrophic chondrocyte marker commonly elevated during in vitro chondrogenesis, and non-chondrogenic markers collagen I, versican and osteonectin. The PCR reactions and detection were performed with the 7500 Fast Real Time PCR system (Applied Biosystems), and the PCR Miner algorithm was used to correct for variation in sample amplification efficiencies [35]. RNA expression levels were normalized to 18S ribosomal RNA and expressed as fold difference over day 0 pure fibrin gels.

2.9. Statistical analyses

All data are presented as the mean ± standard error of the mean. Tensile properties (n=6/group) were analyzed using one factor (group) general linear models (GLMs) with Tukey's test for pairwise comparisons. Results from biochemical analyses and RT-PCR (n=4/group/time point) were analyzed with two factor (group, day) GLMs, and diameters were analyzed with a three factor (group, day, cellular/acellular) GLM. Bonferroni's test was used for pairwise comparisons for multifactor analyses. Relationships across gel groups among the expression levels of the genes at each time point were examined via Pearson's correlation. Significance was at $p<0.05$, and statistical analyses were performed with Minitab (Version 16, Minitab, Inc., State College, PA).

3. Results

3.1. Distribution of fibrin and alginate in different gel groups

Fast Green stained fibrin green, while Safranin-O stained alginate orange or red (due to the negative charge of the alginate), allowing visualization of the architectures across the range of blend ratios (Fig. 1). FA 49:1 and FA 45:4 groups with relatively low concentrations of alginate demonstrated isolated alginate regions within a bulk, interconnected fibrin network. FA 35:12 and FA 30:16 groups with relatively high concentrations of alginate demonstrated an opposite pattern, with isolated fibrin regions within a bulk, interconnected alginate network. FA 43:6 and FA 40:8 groups with intermediate concentrations of alginate and fibrin demonstrated mixed morphologies with interconnected structures of both components. These observations demonstrate an ability to produce a wide range of scaffold architectures by manipulating the ratio of fibrin to alginate.

3.2. Tensile Properties

Pure alginate gels demonstrated a greater tensile modulus (Fig. 2A) than all fibrin-incorporating groups ($p<0.0001$). Among the blended gel groups, FA 49:1 demonstrated a higher tensile modulus than pure fibrin ($p=0.0001$) and all other blended groups ($p\leq0.0002$). Groups with relatively high alginate contents (FA 35:12 and FA 30:16) had significantly lower tensile moduli than all other groups ($p\leq0.0025$ and $p<0.0001$, respectively). Pure fibrin gels had a significantly higher critical tensile strain (Fig. 2B) than pure alginate gels ($p=0.0002$). Among blended gels, the critical strain generally decreased with decreasing fibrin:alginate ratio. Blended gels incorporating relatively low fractions of alginate and demonstrating interconnected fibrin morphologies (FA 49:1 and FA 45:4) were the most extensible, with critical strains significantly greater than those of any other groups (both $p<0.0001$). Gels with intermediate compositions and a mixed morphology (FA 43:6 and FA 40:8 groups) had critical strains significantly greater than that of pure alginate ($p\leq0.01$) but not significantly different from that of pure fibrin, while gels with relatively low fibrin contents and an interconnected alginate morphology (FA 35:12 and FA 30:16) had critical strains significantly lower than that of pure fibrin ($p\leq0.0042$) but not significantly different from that of pure alginate. Therefore, in terms of maintaining gel extensibility which is not lower than that of pure fibrin, the blended groups FA 49:1, FA 45:4, FA 43:6 and FA 40:8 were favorable. Culture experiments were conducted with pure fibrin, pure alginate, and blended groups FA 45:4, FA 40:8 and FA 30:16, which are representative of each of the distinct groupings of morphology and mechanical properties.

3.3. Gel diameter changes

Diameters of acellular gels (Fig. 3A) were fairly stable and decreased significantly between days 14 and 28 only for the FA 40:8 and FA 30:16 groups ($p\leq0.0005$), with day 14 diameters ranging from 92.0 ± 1.1% (FA 45:4) to 99.8 ± 0.07% (FA 40:8) of the average initial diameter and day 28 diameters ranging from 90.8 ± 0.7% (FA 45:4) to 96.7 ± 0.5% (alginate) of the average initial diameter. Cellular gels generally demonstrated a greater diameter reduction than acellular gels (Fig. 3B), with day 14 diameters ranging from 42.4 ± 0.5% (fibrin) to 99.4 ± 0.3% (alginate) of the average initial diameter and day 28 diameters ranging from 41.1 ± 2.3% (fibrin) to 93.6 ± 0.9% (FA 40:8) of the average initial diameter. Among cellular gels, diameters of FA 30:16 and pure alginate groups decreased significantly between day 14 and day 28 ($p=0.0001$). Incorporation of alginate reduced the degree of gel shrinkage for cellular gels, as the diameters of all alginate-containing groups were significantly greater than those of fibrin on both day 14 and day 28 ($p=0.0001$). Compared to cellular alginate gels, the diameters of pure fibrin and FA 45:4 gels were significantly lower on day 14 ($p=0.0001$), and the diameters of pure fibrin, FA 45:4 and FA 30:16 gels were significantly lower on day 28 ($p\leq0.0034$). Cellular gels had significantly smaller diameters

than acellular gels for pure fibrin and FA 45:4 at day 14 (p=0.0001) and for all groups except FA 40:8 at day 28 (p≤0.022). In terms of maintaining the gel dimensional stability, the FA 40:8 and alginate groups were most favorable.

3.4. DNA and sGAG contents

The construct DNA content varied among blend ratios and with culture time (Fig. 4). Pure fibrin gels and gels with a high (FA 45:4) or an intermediate (FA 40:8) concentration of fibrin had higher DNA contents than gels with a low (FA 30:16) fibrin concentration or pure alginate (p≤0.0077). Across all groups, the DNA contents decreased significantly between days 14 and 28 (p<0.0001), but did not fall below the initial (day 0) levels. While groups with higher fibrin content stimulated greater initial proliferation, all groups were favorable in terms of maintaining cell viability and encouraging proliferation relative to day 0 levels.

The total sGAG production (sum of construct and media levels) and fractional retention within the constructs also varied among blend ratios and with time (Fig. 4b). Across groups, the total sGAG production (sum of sGAG in construct plus cumulative sGAG released to media) increased from day 14 to day 28 (p≤0.0001), although the sGAG production in the second two weeks was lower than in the first two weeks for all alginate-incorporating groups. Pure fibrin constructs had lower total sGAG production than any alginate-incorporating groups (p<0.0001), while the FA 40:8 group had higher total sGAG production than any other group (p≤0.0001). Most of the sGAG produced in the first two weeks was retained within the constructs, with fractional retention in alginate-incorporating groups ranging from 95.6 ± 0.6% (FA 30:16) to 99.1 ± 0.3% (alginate), and significantly lower (p≤0.03) fractional sGAG retention of 84.6 ± 1.4% for fibrin. While cumulative production increased from day 14 to day 28, there were no significant differences in construct sGAG contents between day 14 and day 28. Fractional sGAG retention decreased significantly from day 14 to day 28 for all groups (p≤0.0005). The day 28 fractional sGAG retention of 21.5 ± 0.7% in fibrin was significantly lower than in all other groups (p<0.0001), which ranged from 65.7 ± 3.8% (FA 30:16) to 81.2 ± 1.9% (FA 40:8). The resulting construct sGAG per DNA (Fig. 4c) was significantly lower for pure fibrin than for any alginate-incorporating group (p<0.0001), with no significant differences among other groups. The sGAG/DNA increased significantly from day 14 to day 28 (p=0.015), primarily due to the decreases in DNA content (Fig. 4a). Overall, all alginate-incorporating groups were favorable in terms of facilitating sGAG production and retaining sGAG within the constructs.

3.5. Immunofluorescence staining

Immunofluorescence staining of collagen II (Fig. 5a) and the G3 domain of aggrecan (Fig. 5b), two important markers for chondrogenic differentiation, revealed varying patterns of matrix accumulation. On day 28, the pure alginate group had the strongest staining for collagen II, while the pure fibrin group had the weakest collagen II staining. Similarly, aggrecan G3 staining was strongest in pure alginate and weakest in pure fibrin. The blended groups demonstrated mixed populations of cells with different levels of collagen II staining, suggesting (although not definitively demonstrating) that cells may have undergone different degrees of chondrogenic differentiation in different regions of the blended hydrogels. Among the blended gels, the FA 45:4 group showed a relatively weak staining of collagen II and aggrecan G3. Therefore, in terms of supporting collagen II and aggrecan production, FA 40:8, FA 30:16 and alginate groups were favorable.

Images of the actin cytoskeleton (Fig. 5c) revealed various cell morphologies in different gel groups. BM-MSCs in pure fibrin gels displayed spread and irregular morphologies, whereas cells in pure alginate gels displayed rounded cell shapes. Blended gels displayed mixtures of

irregular and rounded cell morphologies. The different sizes or shapes of cell nuclei could be due to different fractions of the cells captured in each image (8 μm/section), but are likely related to the differences in cell morphologies among gel types.

3.6. Gene expression

Alginate promoted stronger expression of chondrogenic genes (collagen II, aggrecan, Sox9) [23] than fibrin, with generally intermediate values for blended scaffolds (Fig. 6). Alginate gels exhibited a higher relative expression of collagen IIa (Fig. 6A) on both day 14 and day 28 than did any fibrin-incorporating group ($p<0.0001$). Collagen IIa expression increased significantly between day 14 and day 28 for pure alginate ($p=0.0004$) but did not significantly change for any other group. Aggrecan expression (Fig. 6B) on day 14 was significantly higher for FA 40:8, FA 30:16 and pure alginate groups than for FA 45:4 or pure fibrin groups ($p<0.0001$). Aggrecan expression decreased significantly from day 14 to day 28 in FA 40:8 and FA 30:16 groups ($p\leq0.0003$), indicating that aggrecan gene expression peaked earlier in groups with an intermediate or a high concentration of alginate. By day 28, aggrecan expression was significantly lower in all fibrin-incorporating groups than in pure alginate ($p\leq0.04$). Relative expression of the transcription factor Sox9 (Fig. 6C), an early marker of chondrogenic differentiation [23], was significantly higher in pure alginate than in any fibrin-incorporating group on both day 14 ($p<0.0001$) and day 28 ($p\leq0.03$). Sox9 expression increased significantly between day 14 and day 28 in fibrin and FA 45:4 groups ($p\leq0.0001$), perhaps indicating a delayed onset of chondrogenesis in groups with high concentrations of fibrin. Relative expression of collagen X (Fig. 6D), a hypertrophic cartilage marker [23], was significantly higher in pure alginate than in any fibrin-incorporating group on day 14 ($p\leq0.0001$). From day 14 to day 28, collagen X expression decreased significantly in alginate and FA 30:16 groups ($p\leq0.0009$) and increased significantly in fibrin and FA 45:4 groups ($p\leq0.0014$). As a result, collagen X expression at day 28 was significantly greater in fibrin than in any blended group ($p\leq0.0003$).

Expression of non-chondrogenic genes also varied substantially with gel composition and culture time. Relative expression of collagen I (Fig. 6E) was significantly higher in alginate than in any fibrin-incorporating group on day 14 ($p<0.0001$). Between day 14 and day 28, collagen I gene expression increased significantly in pure fibrin ($p<0.0001$), but decreased significantly in FA 40:8, FA 30:16 and alginate groups ($p\leq0.0022$). Versican is a marker mainly associated with fibroblasts [36], although it is also expressed in articular cartilage at levels much lower than aggrecan [37]. Relative expression of versican (Fig. 6F) at day 14 was significantly greater in FA 40:8, FA 30:16 and pure alginate groups than in fibrin ($p\leq0.0079$). From day 14 to day 28, versican expression significantly decreased in FA 40:8, FA 30:16 and pure alginate groups ($p\leq0.040$), with no significant differences among gel groups at day 28. The relative expression of osteonectin (Fig. 6G), an osteogenic marker [38], did not vary significantly among groups on day 14, but decreased substantially by day 28 in FA 30:16 and pure alginate groups ($p\leq0.027$) to levels significantly lower than those in fibrin or FA 45:4 groups ($p\leq0.0043$).

Although not a complete measure of the chondrocytic phenotype, the ratio of collagen II:collagen I expression is often used as a rough indicator of the degree of chondrogenesis. The ratio of collagen II:collagen I (Fig. 6H) did not significantly vary among gel groups at day 14. This ratio significantly increased from day 14 to day 28 for alginate ($p=0.029$) and FA 30:16 ($p<0.0001$) groups. At day 28, the collagen II:collagen I ratio was greater for FA 30:16 than for any other group ($p<0.0001$), and was greater for alginate than for FA 45:4 or fibrin groups ($p\leq0.0084$). Taken together, the gene expression data indicate that gels with high alginate contents best promote chondrocytic gene expression and suppress non-chondrocytic gene expression.

Correlations across gel groups revealed strong relationships among some of the genes examined during the process of in vitro chondrogenesis (Table 3). At day 14, expression of the transcription factor Sox9 correlated very strongly with collagen X (R=0.979, $p<0.001$), collagen II (R=0.912, $p<0.001$) and collagen I (R=0.850, $p<0.001$). By day 28 these correlations were weaker but still significant (R=0.687, 0.601 and 0.700, respectively, $p\leq0.005$). Collagen I expression correlated significantly with collagen II (R=0.865, $p<0.001$) and aggrecan (R=0.695, $p=0.001$) at day 14 but not at day 28. Similarly, aggrecan expression correlated significantly with versican expression at day 14 (R=0.749, $p<0.001$) but not at day 28. At day 28, aggrecan expression was positively correlated with collagen II expression (R=0.763, $p<0.001$) and negatively correlated with osteonectin expression (R= −0.704, $p=0.001$).

4. Discussion

In the current study, fibrin/alginate blended hydrogels with various blend ratios were characterized based on physical characteristics and their support of *in vitro* BM-MSC chondrogenesis. The final concentrations of fibrinogen used in fibrin-incorporating gels varied from 30–50 mg/mL, while the final concentrations of alginate in alginate-incorporating gels varied from 1–20 mg/mL. The baseline fibrinogen concentration of 50mg/mL follows from our previous studies using fibrin gels for culture of chondrocytes, fibrochondrocytes and MSCs [13, 29]. Fibrin gels with fibrinogen concentrations below 25 mg/mL may not be sufficiently stable in long-term culture [39], whereas fibrinogen is difficult fully solubilize at concentrations higher than 100 mg/mL (which, when mixed 1:1 with the cell suspension, results in a 50mg/mL solution). Similarly, alginate solutions prepared at concentrations higher than 40 mg/mL are too viscous to pipette and mix well with fibrinogen or cell solutions. While the blend ratios selected for this study do not represent the full range of possible scaffold compositions, they do provide insights into the influence of blend composition on the architecture, physical properties, and biological characteristics of these blended scaffolds.

Fast Green and Safranin-O effectively stained fibrin and alginate, respectively, and the contrast of green and red offered clear visualization of the gel architecture and phase separations between the two materials. When the ratio of fibrin to alginate decreased, the fibrin architecture transitioned from bulk (FA 49:1, FA 45:4) to fibrous (FA 43:6, FA 40:8) and finally to spherical (FA 35:12, FA 30:16) structures against a background of alginate (Fig. 1), with opposing trends in the alginate architecture. Alginate gels through the reaction of sodium alginate with cations (in this case, calcium ions), which bind to the L-guluronic acid subunits of alginate [22]. Fibrinogen is polymerized into fibrin through the cleavage by thrombin, resulting in the exposure of two polymerization sites in the N terminal of the α and β chains and leading to the formation and aggregation of protofibrils into thicker, branched fibrin fibers [40]. The phase separation observed in blended gels indicates that the cross-linking interaction in each individual polymer is stronger than the calcium-mediated cross-linking interaction between fibrin and alginate [41], which resulted in phase separation to reach thermodynamic equilibrium.

Although all fibrin-incorporating groups had lower tensile moduli than pure alginate (Fig. 2A), gels with high (FA 49:1, FA 45:4) or intermediate (FA 43:6, FA 40:8) fibrin concentrations demonstrated higher ultimate tensile strains than alginate (Fig. 2B), which indicates gels with interconnected fibrin structures had high extensibilities, making them suitable for future studies on tensile loading-driven fibrochondrogenesis. The high tensile modulus in FA 49:1 and high critical tensile strains in FA 49:1 and FA 45:4 compared to those of pure fibrin may be due to the exposure of these blended gels to calcium during gel polymerization, which can reinforce the fibrin network formation through binding to the γ

chain of fibrinogen [40]. The focus of these measurements was on evaluation of the initial mechanical behaviors of the constructs, particularly in terms of their suitability for future tensile mechanical stimulation studies. The properties of the constructs would be expected to change with time, particularly if the cells elaborate substantial levels of ECM, and monitoring of mechanical properties will be an important consideration in further studies with blended hydrogels.

Fibrin is a natural component of the provisional scaffold in wound healing and has been widely explored as a scaffold for tissue engineering applications [42], including MSC-based cartilage tissue engineering [13, 20, 21, 43]. One limitation of fibrin, particularly *in vitro*, is suboptimal physical integrity due to cell-mediated degradation and gel contraction. A variety of approaches have been explored to stabilize or stiffen fibrin scaffolds *in vitro*, including the use of fibronolytic inhibitors [31, 44], genipin cross-linking [45, 46], and chemical modification with polyethylene glycol [47]. Interestingly, although similar approaches have been employed to enhance long-term fibrin stability *in vivo* to meet specific clinical needs [45, 48, 49], fibrinolysis is not consistently a barrier to *in vivo* use of fibrin glue or gels for treating cartilage defects [50–53]. Although we attempted to minimize gel degradation by adding the fibrinolytic inhibitor aprotinin to the culture medium, fibrinolysis and cell contraction both likely contributed to the dramatic shrinkage in gels with high fibrin contents. In this study, cellular gels of pure fibrin or with a high fibrin concentration (FA 45:4) shrank substantially during cell culture as evidenced by the progressive decreases in diameter (Fig. 3), and this shrinkage can be attributed to cellular activity since acellular fibrin gels maintained 91% of their original diameters over 28 days. In previous studies [13], physically constraining fibrin gels seeded with bovine BM-MSCs maintained the gel dimension, but increased the release of sGAG to the media. In this study, incorporation of alginate through a simple blending procedure at an intermediate (FA 40:8) or high (FA 30:16) concentration significantly reduced gel contraction. As this was itself unlikely to prevent cell-mediated fibrinolysis or gel contraction, it appears that including enough alginate to achieve an interconnected network was able to physically stabilize the overall construct. This effect is unlikely to be limited to alginate, and further exploration of blended fibrin hydrogels with other reinforcing materials may produce scaffolds suitable for a range of *in vitro* and *in vivo* studies.

Interactions between BM-MSCs and their local microenvironment are an integral part of signaling control of cell attachment, proliferation and differentiation. BM-MSCs in pure fibrin gels demonstrated a more spread morphology, in contrast to a more rounded chondrocyte-like cell shape in pure alginate gels (Fig. 6), with some evidence of intermediate or mixed morphologies in blended gels, indicating that fibrin promoted cell adhesion and spreading. In addition, BM-MSCs cultured in gels with a relatively high fibrin content (pure fibrin, FA 45:4, FA 40:8) showed higher DNA contents than those cultured in gels with a lower fibrin content (FA 30:16) on both day 14 and day 28 ($p \leq 0.0147$) (Fig. 4). We did not directly examine rates of cell proliferation or death, and it is possible that the patterns of DNA content could be influenced by the presence of dead cells prior to the point of DNA degradation. We believe that it is more likely, however, that increased proliferation in gels with high fibrin contents is responsible for this outcome. The integrin adhesion sequence arginine-glycine-aspartic acid (RGD)[54], present in natural ECM materials such as fibrin but absent from alginate, promotes cell attachment and proliferation, and we have previously found greater BM-MSC proliferation in RGD-modified alginate than in non-adhesive control gels [55].

Pure fibrin constructs had the lowest gene expression levels of aggrecan and versican, as well as the lowest production and retention of sGAG within the constructs. Fibrin gels also had the lowest expression of collagen II and maintained low values of the collagen

II:collagen I ratio through 28 days, indicating that pure fibrin hydrogels do not effectively support induction of BM-MSC chondrogenesis by chondrogenic media supplements. In contrast, alginate was superior to fibrin hydrogel in terms of promoting BM-MSC chondrogenesis, based on sGAG production and accumulation, aggrecan and collagen II localization, enhancement of collagen II, aggrecan and Sox9 gene expression, and suppression of non-chondrogenic gene expression. Like the differences in cell attachment and proliferation, these differences in supporting cartilage ECM production between alginate and fibrin gels may also be due to their different cell-scaffold adhesive interactions. Previous studies on bovine BM-MSC chondrogenesis found that conjugation of the RGD sequence to alginate or agarose promoted cell adhesion but inhibited sGAG production [27, 55], with indications that changes in cytoskeletal organization and/or cell shape played a role. Of note, the inhibitory effects of fibrin on chondrogenesis persisted even through 28 days of culture. Although cellular interactions with newly synthesized ECM molecules may overshadow interactions with the fibrin after the early stages of culture, this finding suggests that initial cell-scaffold interactions are sufficient to alter the differentiation of BM-MSCs.

Interestingly, the strong correlations across groups among many of the genes examined (Table 3) suggest that the gel environment did play a strong role in modulating the differentiated phenotype. Responses in blended hydrogels were generally intermediate between those of pure fibrin and pure alginate. While strategies to engineer articular cartilage generally seek to maximize chondrogenic gene expression and cartilage-like matrix deposition, scaffolds producing intermediate patterns of gene expression and matrix production may be more suitable for fibrocartilage tissue engineering. Although the blend ratio producing maximal effects varied among outcome measures, blended gels with moderate alginate concentrations general produced more favorable outcomes in this study. In particular, the FA 40:8 group had the most favorable balance of cell proliferation, sGAG accumulation, gene expression, and mechanical properties. It should be noted that these findings differ from those of a recent study reporting inferior BM-MSC chondrogenesis in fibrin-alginate composite beads versus pure fibrin beads, with decreased cell survival, ECM production and chondrogenic gene expression with the addition of 0.3% or 0.6% alginate to 30 mg/mL fibrin hydrogels [56]. This disparity may be due to differences in the polymerization conditions, which can substantially influence the microstructure and mechanical properties of fibrin/alginate blends [41]. Of some concern, the DNA content decreased in all groups between 14 and 28 days, and no groups exhibited increased sGAG deposition between 14 and 28 days. Further investigation of the influences of cell-scaffold adhesive interactions and gel architecture on BM-MSC differentiation may lead to scaffolds that better promote cell survival, differentiation, and functional ECM assembly, allowing the design of blended scaffolds suitable for a wide range of applications.

Interestingly, while the focus of this study was initially on the development of appropriate scaffolds for mechanical loading studies, the results have bearing on the ability to produce engineered tissues with spatially heterogeneous cellular phenotypes and ECM compositions. Immunofluoresence staining demonstrated regional variations in the ECM proteins within each blended gel (Fig. 6), indicating that blended hydrogels support the formation of heterogeneous structures with different matrix constituents. While we did not directly associate heterogeneous patterns of matrix deposition with local variations in gel composition, these patterns suggest that BM-MSCs underwent differing degrees of chondrogenesis in different regions of the blended gels, depending on the local composition of the scaffold. Interestingly, in blended gels the transcript levels for most of the genes examined were intermediate between those of pure fibrin and pure alginate. While this might be related to uniform differences in responses throughout the entire construct, the spatial variations in ECM protein accumulation and cell morphology suggests that the bulk responses in blended likely represent an averaging of distinct subpopulations residing in the

different materials. These results suggest that the local environmental cues from the scaffold were able to maintain distinct cell behaviors in close proximity to regions with different cell/matrix characteristics, suggesting that spatial patterning of BM-MSC differentiation at relatively small length scales may be feasible. While the simple blending approach taken in the current study produces a range of macroscopic gel architectures, the production of predetermined, repeatable microstructural features would require more advanced three-dimensional deposition strategies. In the future, we envision the coordinated manipulation of the cell-scaffold interaction, the biochemical and mechanical cues to guide the formation of fibrocartilaginous tissue with desired cell and matrix constituents for fibrocartilage repair.

5. Conclusions

Fibrin/alginate blended hydrogels at various blend ratios were successfully fabricated and evaluated based on the following criteria: critical tensile strain, dimensional stability, DNA content, sGAG production, Collagen II and aggrecan G3 staining, and gene expression of chondrogenic and non-chondrogenic genes. Pure fibrin and pure alginate gels showed distinctive capabilities mechanically and biologically in supporting BM-MSC chondrogenic differentiation. Fibrin promoted cell proliferation and gel extensibility, while alginate improved the gel biostability. For chondrogenesis, alginate was superior to fibrin in terms of increasing sGAG and collagen II production, promoting chondrogenic gene and suppressing non-chondrogenic gene expression. Blending the two materials at different ratios allowed us to produce a range of cellular constructs with various mechanical and biological properties. Of the blends examined, FA 40:8 appeared to be the most appropriate group for future studies on tensile loading-driven BM-MSC fibrochondrogenesis. As MSC differentiation varied between fibrin and alginate regions, control of gel architecture by manipulating the blend ratio may allow development of heterogeneous engineered tissues. Therefore, this study not only examines the mechanical and biological properties of different gel systems for supporting BM-MSC chondrogenesis, but also provides insight into the development of heterogeneous engineered tissues by control of the cell-scaffold interactions through manipulating the scaffold composition.

Acknowledgments

We thank Khang Dinh, Min-Sun Son, Carrie Hang-Yin Ling and Janice Lai for their technical assistance and suggestions on gel fabrication, RT-PCR and tensile tests, respectively. This study was supported by the grant R01AR054939 from NIAMS/NIH, the funding from Stanford Mechanical Engineering Summer Undergraduate Research Institute (SURI) Program and an Arthritis Foundation Postdoctoral Fellowship (fellowship recipient: Dr. Kun Ma).

Role of the Funding Source

The study sponsors had no role in the design, execution or interpretation of the study, in the writing of the paper, or in the decision to submit the paper for publication.

References

1. Ibarra C, Koski JA, Warren RF. Tissue engineering meniscus: cells and matrix. Orthop Clin North Am. 2000; 31:411–8. [PubMed: 10882467]
2. Messner K, Gao J. The menisci of the knee joint. Anatomical and functional characteristics, and a rationale for clinical treatment. J Anat. 1998; 193 (Pt 2):161–78. [PubMed: 9827632]
3. Kambic HE, McDevitt CA. Spatial organization of types I and II collagen in the canine meniscus. J Orthop Res. 2005; 23:142–9. [PubMed: 15607886]
4. Melrose J, Smith S, Cake M, Read R, Whitelock J. Comparative spatial and temporal localisation of perlecan, aggrecan and type I, II and IV collagen in the ovine meniscus: an ageing study. Histochemistry and cell biology. 2005; 124:225–35. [PubMed: 16028067]

5. Valiyaveettil M, Mort JS, McDevitt CA. The concentration, gene expression, and spatial distribution of aggrecan in canine articular cartilage, meniscus, and anterior and posterior cruciate ligaments: a new molecular distinction between hyaline cartilage and fibrocartilage in the knee joint. Connect Tissue Res. 2005; 46:83–91. [PubMed: 16019418]
6. Vanderploeg EJ, Wilson CG, Imler SM, Ling CH, Levenston ME. Regional variations in the distribution and colocalization of extracellular matrix proteins in the juvenile bovine meniscus. J Anat. 2012 In press.
7. Hellio Le Graverand MP, Ou Y, Schield-Yee T, Barclay L, Hart D, Natsume T, et al. The cells of the rabbit meniscus: their arrangement, interrelationship, morphological variations and cytoarchitecture. J Anat. 2001; 198:525–35. [PubMed: 11430692]
8. Son M, Levenston ME. Discrimination of meniscal cell phenotypes using gene expression profiles. Eur Cell Mater. 2012; 23:195–208. [PubMed: 22442006]
9. McDermott I. Meniscal tears, repairs and replacement: their relevance to osteoarthritis of the knee. Br J Sports Med. 2011; 45:292–7. [PubMed: 21297172]
10. Tenuta JJ, Arciero RA. Arthroscopic evaluation of meniscal repairs. Factors that effect healing. Am J Sports Med. 1994; 22:797–802. [PubMed: 7856804]
11. Muraglia A, Cancedda R, Quarto R. Clonal mesenchymal progenitors from human bone marrow differentiate in vitro according to a hierarchical model. J Cell Sci. 2000; 113 (Pt 7):1161–6. [PubMed: 10704367]
12. Pittenger MF, Mackay AM, Beck SC, Jaiswal RK, Douglas R, Mosca JD, et al. Multilineage potential of adult human mesenchymal stem cells. Science. 1999; 284:143–7. [PubMed: 10102814]
13. Connelly JT, Vanderploeg EJ, Mouw JK, Wilson CG, Levenston ME. Tensile loading modulates bone marrow stromal cell differentiation and the development of engineered fibrocartilage constructs. Tissue Eng Part A. 2010; 16:1913–23. [PubMed: 20088686]
14. Lee, CH.; Sun, JY.; Mao, JJ. Fibrochondrocytes as potential therapeutic cells from human mesenchymal cells. TERMIS-NA 2010 Annual Conference & Exposition; 2010. p. 378
15. Leddy HA, Awad HA, Guilak F. Molecular diffusion in tissue-engineered cartilage constructs: effects of scaffold material, time, and culture conditions. J Biomed Mater Res B Appl Biomater. 2004; 70:397–406. [PubMed: 15264325]
16. Baker BM, Nathan AS, Gee AO, Mauck RL. The influence of an aligned nanofibrous topography on human mesenchymal stem cell fibrochondrogenesis. Biomaterials. 2010; 31:6190–200. [PubMed: 20494438]
17. Kim IL, Mauck RL, Burdick JA. Hydrogel design for cartilage tissue engineering: a case study with hyaluronic acid. Biomaterials. 2011; 32:8771–82. [PubMed: 21903262]
18. Bhardwaj N, Nguyen QT, Chen AC, Kaplan DL, Sah RL, Kundu SC. Potential of 3-D tissue constructs engineered from bovine chondrocytes/silk fibroin-chitosan for in vitro cartilage tissue engineering. Biomaterials. 2011; 32:5773–81. [PubMed: 21601277]
19. van Susante JL, Buma P, Schuman L, Homminga GN, van den Berg WB, Veth RP. Resurfacing potential of heterologous chondrocytes suspended in fibrin glue in large full-thickness defects of femoral articular cartilage: an experimental study in the goat. Biomaterials. 1999; 20:1167–75. [PubMed: 10395385]
20. Park JS, Yang HN, Woo DG, Jeon SY, Park KH. Chondrogenesis of human mesenchymal stem cells in fibrin constructs evaluated in vitro and in nude mouse and rabbit defects models. Biomaterials. 2011; 32:1495–507. [PubMed: 21122912]
21. Ahmed TA, Giulivi A, Griffith M, Hincke M. Fibrin glues in combination with mesenchymal stem cells to develop a tissue-engineered cartilage substitute. Tissue Eng Part A. 2011; 17:323–35. [PubMed: 20799906]
22. Hwang NS, Varghese S, Elisseeff J. Cartilage tissue engineering: Directed differentiation of embryonic stem cells in three-dimensional hydrogel culture. Methods Mol Biol. 2007; 407:351–73. [PubMed: 18453267]
23. Xu J, Wang W, Ludeman M, Cheng K, Hayami T, Lotz JC, et al. Chondrogenic differentiation of human mesenchymal stem cells in three-dimensional alginate gels. Tissue Eng Part A. 2008; 14:667–80. [PubMed: 18377198]

24. Mauck RL, Soltz MA, Wang CC, Wong DD, Chao PH, Valhmu WB, et al. Functional tissue engineering of articular cartilage through dynamic loading of chondrocyte-seeded agarose gels. J Biomech Eng. 2000; 122:252–60. [PubMed: 10923293]
25. Connelly JT, Wilson CG, Levenston ME. Characterization of proteoglycan production and processing by chondrocytes and BMSCs in tissue engineered constructs. Osteoarthritis Cartilage. 2008; 16:1092–100. [PubMed: 18294870]
26. Perka C, Spitzer RS, Lindenhayn K, Sittinger M, Schultz O. Matrix-mixed culture: new methodology for chondrocyte culture and preparation of cartilage transplants. J Biomed Mater Res. 2000; 49:305–11. [PubMed: 10602062]
27. Connelly JT, Garcia AJ, Levenston ME. Interactions between integrin ligand density and cytoskeletal integrity regulate BMSC chondrogenesis. J Cell Physiol. 2008; 217:145–54. [PubMed: 18452154]
28. Sekiya I, Larson BL, Smith JR, Pochampally R, Cui JG, Prockop DJ. Expansion of human adult stem cells from bone marrow stroma: conditions that maximize the yields of early progenitors and evaluate their quality. Stem Cells. 2002; 20:530–41. [PubMed: 12456961]
29. Vanderploeg EJ, Imler SM, Brodkin KR, Garcia AJ, Levenston ME. Oscillatory tension differentially modulates matrix metabolism and cytoskeletal organization in chondrocytes and fibrochondrocytes. J Biomech. 2004; 37:1941–52. [PubMed: 15519602]
30. Demol J, Eyckmans J, Roberts SJ, Luyten FP, Van Oosterwyck H. Does tranexamic acid stabilised fibrin support the osteogenic differentiation of human periosteum derived cells? European cells & materials. 2011; 21:272–85. [PubMed: 21432782]
31. Huang CY, Deitzer MA, Cheung HS. Effects of fibrinolytic inhibitors on chondrogenesis of bone-marrow derived mesenchymal stem cells in fibrin gels. Biomech Model Mechanobiol. 2007; 6:5–11. [PubMed: 16691415]
32. Kim YJ, Sah RL, Doong JY, Grodzinsky AJ. Fluorometric assay of DNA in cartilage explants using Hoechst 33258. Anal Biochem. 1988; 174:168–76. [PubMed: 2464289]
33. Enobakhare BO, Bader DL, Lee DA. Quantification of sulfated glycosaminoglycans in chondrocyte/alginate cultures, by use of 1,9-dimethylmethylene blue. Anal Biochem. 1996; 243:189–91. [PubMed: 8954546]
34. Chomczynski P, Sacchi N. Single-step method of RNA isolation by acid guanidinium thiocyanate-phenol-chloroform extraction. Anal Biochem. 1987; 162:156–9. [PubMed: 2440339]
35. Zhao S, Fernald RD. Comprehensive algorithm for quantitative real-time polymerase chain reaction. J Comput Biol. 2005; 12:1047–64. [PubMed: 16241897]
36. Kawashima H, Li YF, Watanabe N, Hirose J, Hirose M, Miyasaka M. Identification and characterization of ligands for L-selectin in the kidney. I. Versican, a large chondroitin sulfate proteoglycan, is a ligand for L-selectin. Int Immunol. 1999; 11:393–405. [PubMed: 10221651]
37. Grover J, Roughley PJ. Versican gene expression in human articular cartilage and comparison of mRNA splicing variation with aggrecan. Biochem J. 1993; 291 (Pt 2):361–7. [PubMed: 8484718]
38. Gehron Robey P. The biochemistry of bone. Endocrinol Metab Clin North Am. 1989; 18:858–902. [PubMed: 2691241]
39. Eyrich D, Brandl F, Appel B, Wiese H, Maier G, Wenzel M, et al. Long-term stable fibrin gels for cartilage engineering. Biomaterials. 2007; 28:55–65. [PubMed: 16962167]
40. Pratt KP, Cote HC, Chung DW, Stenkamp RE, Davie EW. The primary fibrin polymerization pocket: three-dimensional structure of a 30-kDa C-terminal gamma chain fragment complexed with the peptide Gly-Pro-Arg-Pro. Proc Natl Acad Sci U S A. 1997; 94:7176–81. [PubMed: 9207064]
41. Shikanov A, Xu M, Woodruff TK, Shea LD. Interpenetrating fibrin-alginate matrices for in vitro ovarian follicle development. Biomaterials. 2009; 30:5476–85. [PubMed: 19616843]
42. Ahmed TA, Dare EV, Hincke M. Fibrin: a versatile scaffold for tissue engineering applications. Tissue Eng Part B Rev. 2008; 14:199–215. [PubMed: 18544016]
43. Dickhut A, Gottwald E, Steck E, Heisel C, Richter W. Chondrogenesis of mesenchymal stem cells in gel-like biomaterials in vitro and in vivo. Front Biosci. 2008; 13:4517–28. [PubMed: 18508526]

44. Kupcsik L, Alini M, Stoddart MJ. Epsilon-aminocaproic acid is a useful fibrin degradation inhibitor for cartilage tissue engineering. Tissue Eng Part A. 2009; 15:2309–13. [PubMed: 19086806]
45. Dare EV, Griffith M, Poitras P, Kaupp JA, Waldman SD, Carlsson DJ, et al. Genipin cross-linked fibrin hydrogels for in vitro human articular cartilage tissue-engineered regeneration. Cells Tissues Organs. 2009; 190:313–25. [PubMed: 19287127]
46. Schek RM, Michalek AJ, Iatridis JC. Genipin-crosslinked fibrin hydrogels as a potential adhesive to augment intervertebral disc annulus repair. Eur Cell Mater. 2011; 21:373–83. [PubMed: 21503869]
47. Galler KM, Cavender AC, Koeklue U, Suggs LJ, Schmalz G, D'Souza RN. Bioengineering of dental stem cells in a PEGylated fibrin gel. Regen Med. 2011; 6:191–200. [PubMed: 21391853]
48. Fussenegger M, Meinhart J, Hobling W, Kullich W, Funk S, Bernatzky G. Stabilized autologous fibrin-chondrocyte constructs for cartilage repair in vivo. Ann Plast Surg. 2003; 51:493–8. [PubMed: 14595186]
49. Smith JD, Chen A, Ernst LA, Waggoner AS, Campbell PG. Immobilization of aprotinin to fibrinogen as a novel method for controlling degradation of fibrin gels. Bioconjug Chem. 2007; 18:695–701. [PubMed: 17432824]
50. Silverman RP, Passaretti D, Huang W, Randolph MA, Yaremchuk MJ. Injectable tissue-engineered cartilage using a fibrin glue polymer. Plast Reconstr Surg. 1999; 103:1809–18. [PubMed: 10359239]
51. Peretti GM, Randolph MA, Zaporojan V, Bonassar LJ, Xu JW, Fellers JC, et al. A biomechanical analysis of an engineered cell-scaffold implant for cartilage repair. Ann Plast Surg. 2001; 46:533–7. [PubMed: 11352428]
52. Silverman RP, Bonasser L, Passaretti D, Randolph MA, Yaremchuk MJ. Adhesion of tissue-engineered cartilate to native cartilage. Plast Reconstr Surg. 2000; 105:1393–8. [PubMed: 10744230]
53. Xu JW, Zaporojan V, Peretti GM, Roses RE, Morse KB, Roy AK, et al. Injectable tissue-engineered cartilage with different chondrocyte sources. Plast Reconstr Surg. 2004; 113:1361–71. [PubMed: 15060348]
54. Ruoslahti E, Pierschbacher MD. Arg-Gly-Asp: a versatile cell recognition signal. Cell. 1986; 44:517–8. [PubMed: 2418980]
55. Connelly JT, Garcia AJ, Levenston ME. Inhibition of in vitro chondrogenesis in RGD-modified three-dimensional alginate gels. Biomaterials. 2007; 28:1071–83. [PubMed: 17123602]
56. Ho ST, Cool SM, Hui JH, Hutmacher DW. The influence of fibrin based hydrogels on the chondrogenic differentiation of human bone marrow stromal cells. Biomaterials. 2010; 31:38–47. [PubMed: 19800683]

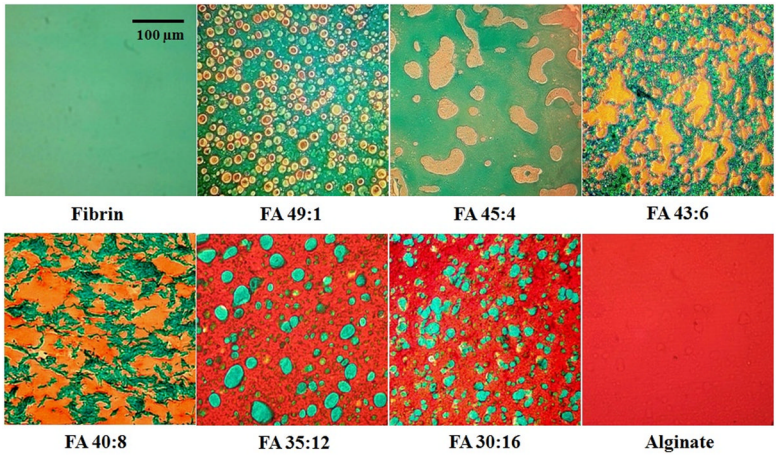

Figure 1.
Staining of fibrin with Fast Green (green) and alginate with Safranin-O (orange/red) in different groups revealed gel architectures that varied with the fibrin:alginate ratio. Scale bar: 100 μm.

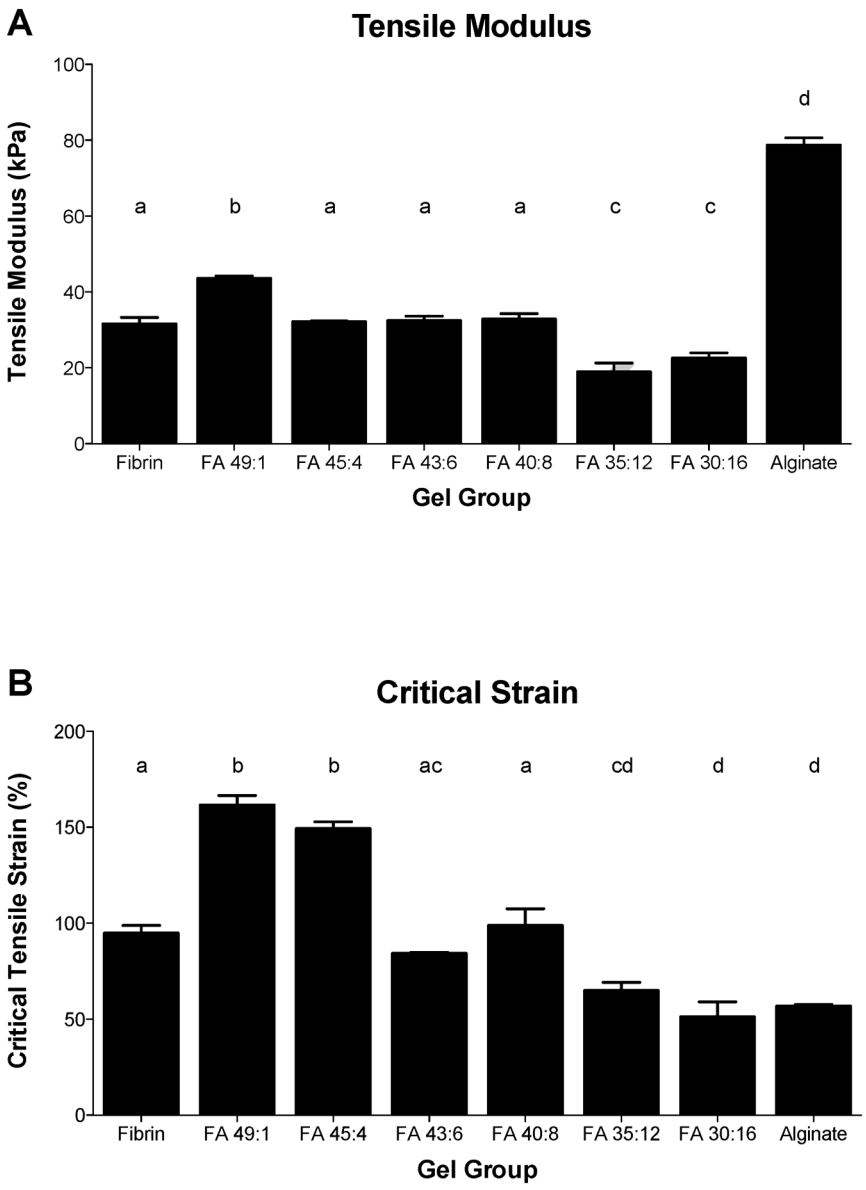

Figure 2.

(A) Tensile modulus and (B) critical tensile strain for different blend ratio groups. Mean ± SEM, n=6/group. Letters indicate significance patterns, with differences at $p<0.05$ between groups with no common labels.

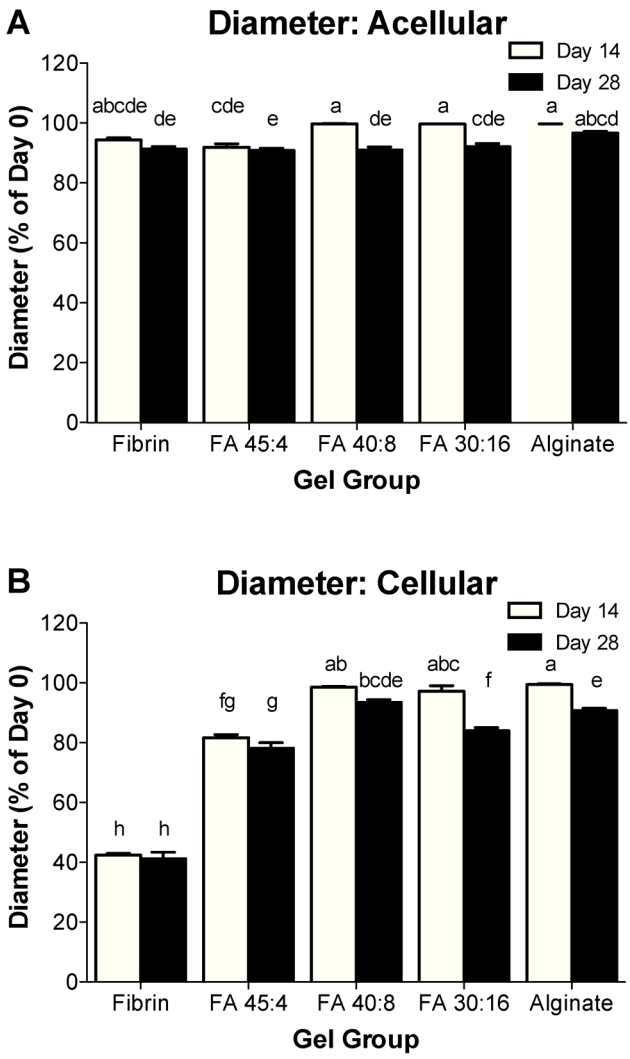

Figure 3.

Gel diameters on day 14 and day 28 for (A) acellular and (B) cellular gels from different blend ratio groups. Mean ± SEM, n=4/group. Letters indicate significance patterns across both acellular and cellular groups, with differences at $p<0.05$ between groups with no common labels.

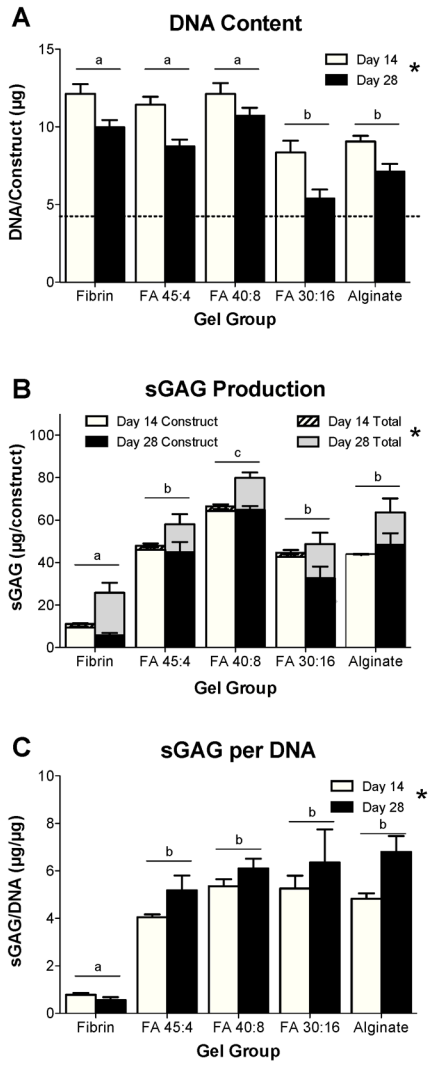

Figure 4.

(A) DNA content, (B) sGAG production and (C) construct sGAG per DNA on day 14 and day 28 for different blend ratio groups. Mean ± SEM, n=4/group. Letters indicate significance patterns, with differences at $p<0.05$ between groups with no common labels. For all three measures, values at day 14 and day 28 were significantly different (*) with no interaction with the gel composition. The dashed line in (A) indicates the average DNA content at day 0. Markers in (B) reflect statistical analyses for total sGAG production (the sum of construct sGAG content and cumulative sGAG released to the culture media), and results for construct sGAG production and fractional retention are described in the text.

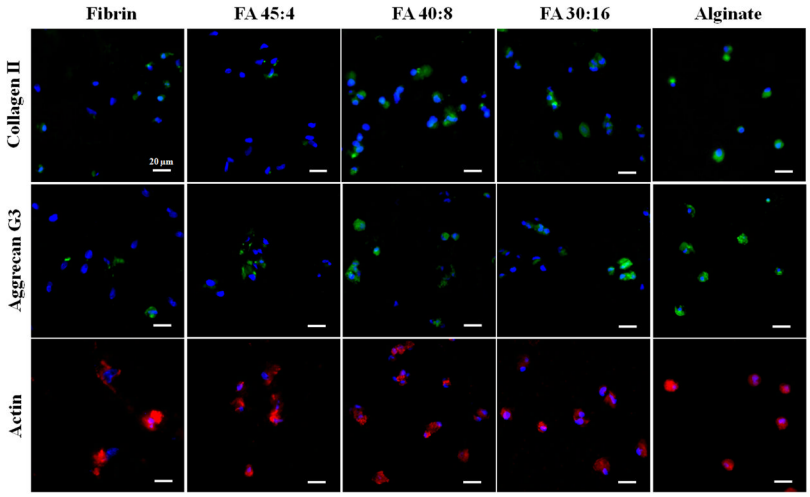

Figure 5.

Immunofluoresence staining of collagen type II (top row), aggrecan G3 (middle row) and actin (bottom row) on day 28 in representative images from different blend ratio groups. Green indicates the targeted protein, red indicates actin and blue indicates nuclear staining by DAPI. Scale bars: 20 μm.

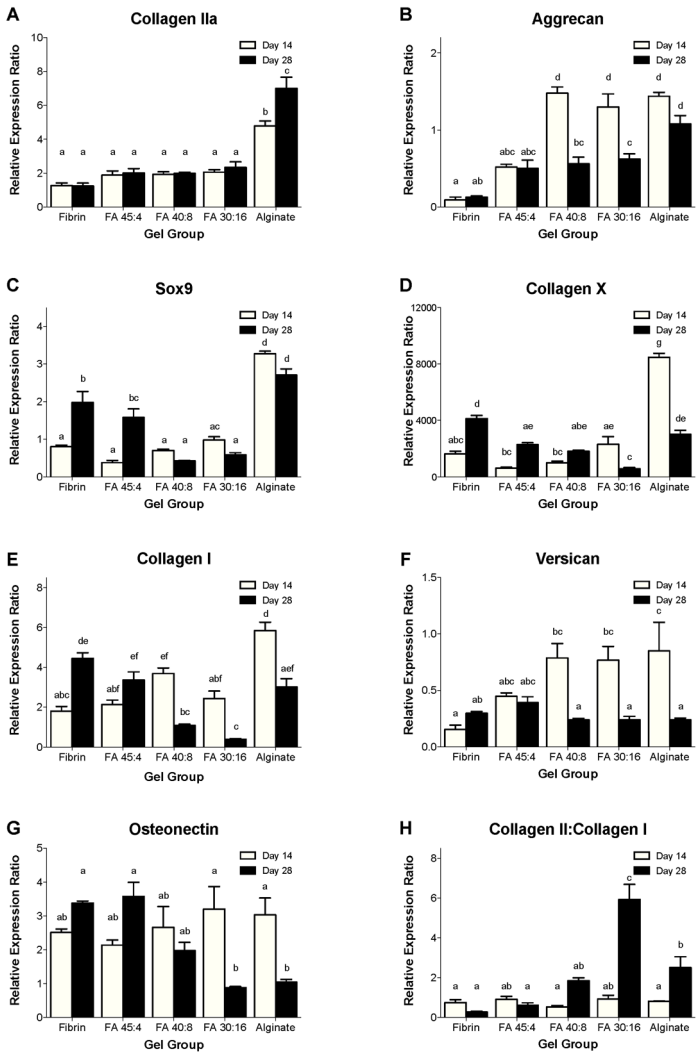

Figure 6.

The relative gene expression ratios (RER) of BM-MSCs from different blend ratio groups on day 14 and day 28 for (A) collagen type II, (B) aggrecan, (C) Sox9, (D) collagen type X, (E) collagen type I, (F) versican, (G) osteonectin and (H) the Collagen II:Collagen I ratio. Data are normalized to 18S rRNA and expressed as fold difference relative to Day 0 fibrin gels. Mean ± SEM, n=4/group. Letters indicate significance patterns, with differences at $p<0.05$ between groups with no common labels.

Table 1

Final concentrations of fibrinogen, thrombin and alginate in the different blend ratio groups. FA X:Y indicates a blend with a final concentration of X mg/mL fibrin and Y mg/mL alginate.

Component	Fibrin	FA 49:1	FA 45:4	FA 43:6	FA 40:8	FA 35:12	FA 30:16	Alginate
Fibrinogen (mg/mL)	50	49	45	43	40	35	30	0
Alginate (mg/mL)	0	1	4	6	8	12	16	20
Thrombin (U/mL)	25	24.5	22.5	21.5	20	17.5	15	0

Table 2

Real time PCR primer sequences.

Target gene	Accession No.	Forward	Reverse
Collagen IIa	NM_001844	5′-TGC AGG ATG GGC AGA GGT AT-3′	5′-CAC AGA CAC AGA TCC GGC AG-3′
Aggrecan	NM_001135	5′-TTC TTG GAG AAG GGA GTC CA-3′	5′-ACA GCT GCA GTG ATG ACC CT-3′
Sox9	NM_000346	5′-GAG GCA GAG GAG GCC ACG GA-3′	5′-CCT GGG ATT GCC CCG AGT GC-3′
Collagen X	NM_000493	5′- CAT AAA AGG CCC ACT ACC CA -3′	5′- GTG GAC CAG GAG TAC CTT GC -3′
Collagen I	NM_000088	5′-AAG AGG AAG GCC AAG TCG AG-3′	5′-CAC ACG TCT CGG TCA TGG TA-3′
Versican	NM_004385	5′-TCT CCC CAG GAA ACT TAC GA-3′	5′-CAC TCT TTT GCA GCC TCC TC-3′
Osteonectin	NM_003118	5′-CTT CAG ACT GCC CGG AGA-3′	5′-GAA AGA AGA TCC AGG CCC TC-3′
18S rRNA	NM_022551	5′-CTT TGC CAT CAC TGC CAT TA-3′	5′-ATC CTC AGT GAG TTC TCC CG-3′

Table 3

Correlations among gene expression levels across all samples at each time point.

Day 14

	Collagen IIa	Aggrecan	Sox9	Collagen X	Collagen I	Versican
Aggrecan	*r*=0.546 *p*=0.013					
Sox9	***r*=0.912** ***p*<0.001**	*r*=0.461 *p*=0.041				
Collagen X	***r*=0.893** ***p*<0.001**	*r*=0.450 *p*=0.046	***r*=0.979** ***p*<0.001**			
Collagen I	***r*=0.865** ***p*<0.001**	*r*=0.695 *p*=0.001	***r*=0.850** ***p*<0.001**	***r*=0.810** ***p*<0.001**		
Versican	*r*=0.461 *p*=0.041	***r*=0.749** ***p*<0.001**	NS	NS	*r*=0.567 *p*=0.009	
Osteonectin	NS	*r*=0.478 *p*=0.033	NS	NS	NS	*r*=0.516 *p*=0.020

Day 28

	Collagen IIa	Aggrecan	Sox9	Collagen X	Collagen I	Versican
Aggrecan	**r=0.763** **p<0.001**					
Sox9	r=0.601 p=0.005	NS				
Collagen X	NS	NS	r=0.687 p=0.001			
Collagen I	NS	NS	**r=0.700** **p=0.001**	**r=0.849** **p<0.001**		

Day 28						
	Collagen IIa	**Aggrecan**	**Sox9**	**Collagen X**	**Collagen I**	**Versican**
Versican	NS	NS	NS	NS	r=0.483 p=0.031	
Osteonectin	r=−0.549 p=0.012	**r=−0.704** **p=0.001**	NS	r=0.519 p=0.019	r=0.633 p=0.003	r=0.650 p=0.002